

## Pattern formation in composite excitable media

M. Bär,<sup>1,2</sup> I. G. Kevrekidis,<sup>1</sup> H.-H. Rotermund,<sup>2</sup> and G. Ertl<sup>2</sup>

<sup>1</sup>Department of Chemical Engineering, Princeton University, Princeton, New Jersey 08544-5263

<sup>2</sup>Fritz-Haber-Institut der Max-Planck-Gesellschaft, Faradayweg 4-6, 14195 Berlin, Germany

(Received 14 August 1995)

The propagation of periodic reaction-diffusion waves (wave trains) on a composite catalytic surface, whose subdomains are characterized by different reaction kinetics, is observed experimentally during CO oxidation and analyzed computationally with a realistic reaction-diffusion model. Complete transmission as well as partial blocking of plane waves, creation of spirals as well as chemical turbulence due to presence of a domain boundary with curved waves are found for different parameters.

PACS number(s): 82.40.Ck

Experiments and theoretical investigations on pattern formation and wave propagation in chemical systems are often motivated by their potential role in the understanding of morphogenesis and functional aspects in biological systems [1]. Although most biological systems are strongly heterogeneous, chemical experiments have mainly been conducted in homogeneous setups. Recently, theoretical [2] and experimental [3] results on the behavior of fronts in heterogeneous media have been obtained. In excitable media that support spirals and pulses, several cases where heterogeneities with different behavior appear on a length scale smaller than or equal to the spiral wavelength in the medium have been studied [4]. Here, we would like to address the opposite case: composite surfaces whose heterogeneities (entire domains) have a length much larger than the typical spiral wavelength. As a simple example of such a composite medium we study theoretically two large rectangular domains with slightly different properties, that possess a common linear interface. We start in one dimension (1D), when the model geometry consists of two line segments with a point interface, and then proceed to two dimensions (2D). Both halves of this composite are excitable media and can sustain pulses and wave trains in 1D as well as rotating spiral waves in 2D [5]. It has been shown recently that a sudden change (e.g., a sharp edge or narrow slit) in the geometry of a no-flux boundary of an excitable medium can give rise to a range of phenomena from wave blocking to spiral creation [6,7]. Here, we deal with a yet different kind of heterogeneity: the influence of spatial variations of *properties* of the medium on the propagation of waves (in this case finite step changes in reactivity). In contrast to the no-flux boundary conditions of the complex geometry examples mentioned above, the type of domain boundary we consider *does* allow for species diffusion across it, and affects the speed and the profile of the *transmitted* wave significantly.

An experimental realization of such a system in the context of catalytic surface reactions has recently been constructed by the coupling of a pure Pt(110) surface with a partially (up to 5%) Au-covered Pt(110) surface [8,9]. The spatiotemporal dynamics of the CO and O concentrations on such a surface have been recorded by means of photoemission electron microscopy (PEEM) [10]. One observation (cf. Fig. 15 of Ref. [9]) shows waves arising from the spiral center and crossing through the boundary, keeping the same

frequency on both sides, while the spatial profile and the length of the alternating black and white areas (indicating oxygen- and CO-rich areas on the surfaces) change drastically; alternatively, in a different experiment, spiral tips form and remain close to the domain boundary (cf. Fig. 16 in [9]).

To get a more systematic understanding of the dynamics close to such a boundary, numerical simulations with a simplified model of the CO oxidation on Pt(110) in the excitable regime [11] have been performed. The model equations read

$$\frac{\partial u}{\partial t} = \frac{1}{\epsilon} u(1-u) \left( u - \frac{w+b(\mathbf{x})}{a} \right) + \nabla^2 u, \quad (1)$$

$$\frac{\partial w}{\partial t} = f(u) - w, \quad (2)$$

with

$$f(u) = \begin{cases} 0 & \text{if } u < \frac{1}{3} \\ 1 - 6.75u(u-1)^2 & \text{if } \frac{1}{3} \leq u \leq 1 \\ 1 & \text{if } u > 1. \end{cases} \quad (3)$$

Here,  $u$  represents the surface coverage and  $w$  the surface structure (degree of  $1 \times 2$ -reconstructed surface) [11]. Note that  $u=0$  corresponds to a CO (O) coverage of 0.65 (0.01) monolayers (ML) and that  $u=1$  represents 0.2 ML (0.25 ML) for CO (O) on the Pt surface.

The dimensionless time and space units of the scaled Eqs. (1)–(3) correspond roughly to 2 s and 1  $\mu\text{m}$ , respectively. The experimental parameters CO partial pressure  $p_{\text{CO}}$ , oxygen partial pressure  $p_{\text{O}_2}$ , and the surface temperature  $T$  have been mapped into the model parameters  $a$ ,  $b$ , and  $\epsilon$  [11]. The drop in the oxygen sticking coefficient due to the presence of the inert gold atoms is stronger than the same effect for carbon monoxide (for a detailed discussion of the influence of gold on the reaction kinetics see [9]). This can be mimicked in the model through a spatial dependency of the parameter  $b(\mathbf{x})$ , which essentially expresses the balance between CO and O on the surface:  $b < 0$  ( $b > 0$ ) indicates a dominance of oxygen (carbon monoxide). Here the specific form

$$b(\mathbf{x}) = \begin{cases} b_1 & \text{if } x \leq L/2 \\ b_2 & \text{if } x > L/2 \end{cases} \quad (4)$$

has been used, where  $L$  denotes the length of the system in the  $x$  direction. The Au atom's influence on the activation energy for CO diffusion and adsorption will be neglected here, since the Au coverages of interest are small. In all images shown below, oxygen- (CO-) rich regions will appear black (white). Equations (1)–(3) are similar to a generic model of excitable media, introduced by Barkley [12]; the following results are therefore expected to hold for a wide class of coupled excitable media.

As representative dynamics we studied the influence of composite “grain” boundaries on traveling pulse trains. In our simulation setup we imposed a source of oxygen waves on the left boundary [realized by a Dirichlet boundary condition  $u(x=0)=w(x=0)=1$ ]. The two diffusionally coupled grains are individually characterized by the existence of a CO-stable rest state on the left side [medium 1 corresponding to the Au-covered Pt(110) surface with  $b_1 > 0$ ], and by an oscillatory or O-stable state on the right [medium 2 representing the “pure” Pt(110) surface with  $b_2 < 0$ ]. At the rightmost edge we use a zero-flux-boundary condition [ $(\partial u/\partial x)(x=L)=(\partial w/\partial x)(x=L)=0$ ]. At fixed  $b_1$  the source creates a stable wave train in medium 1 with a constant period  $\tau_1$ . With increasing  $b_1$ , the period  $\tau_1$  decreases. Then the value of  $b_2$  is varied at fixed  $b_1$ . If  $b_2$  becomes smaller than  $b_{\text{crit},2}$ , waves cease to propagate in medium 2. For larger  $b_2$ , we observe two basic types of behavior. Either every wave of the stable train in medium 1 passes the boundary and adapts to the new conditions (1:1 transmission) or every other wave is blocked (1:2 transmission) as shown in Fig. 1(a). The first case results in equal temporal periods of the wave trains on both sides of the boundary, while in the latter case the period in medium 2 is twice that of medium 1.

The extent of the effect depends strongly on  $b_1$  and the associated period  $\tau_1$ . We plot the regions of different qualitative behavior in two-parameter space ( $\tau_1$  and the threshold  $b_2$ ) in Fig. 1(b). The 1:2 transmission is only seen for sufficiently small period (high incident frequency). The blocking of every other pulse in these cases may be rationalized as follows: When a pulse enters into medium 2, its speed and form need to adapt to the new conditions. While the leading part (front) takes on the new speed, the back is shifted to achieve the new pulse profile. In our case the dark (oxygen-rich) part of the wave expands, as manifested in a delay of the propagation of the wave back. This delay increases the possibility of an interaction with the subsequent incident pulse near the boundary (especially in high frequency wave trains) and may even cause the observed blocking of every second wave. It is important to note that, in the case of blocking here, medium 2 supports usually waves with the period of the incident train, so wave blocking due to a violation of the dispersion relation of medium 2 can be ruled out. The observed transformation at the boundary might also be considered as a response of the boundary to a forcing by the wave train in medium 1; in fact, similar as well as chaotic response patterns have been found in experiments with periodically forced cardiac fibers and in corresponding model calculations (see [13] and references therein).

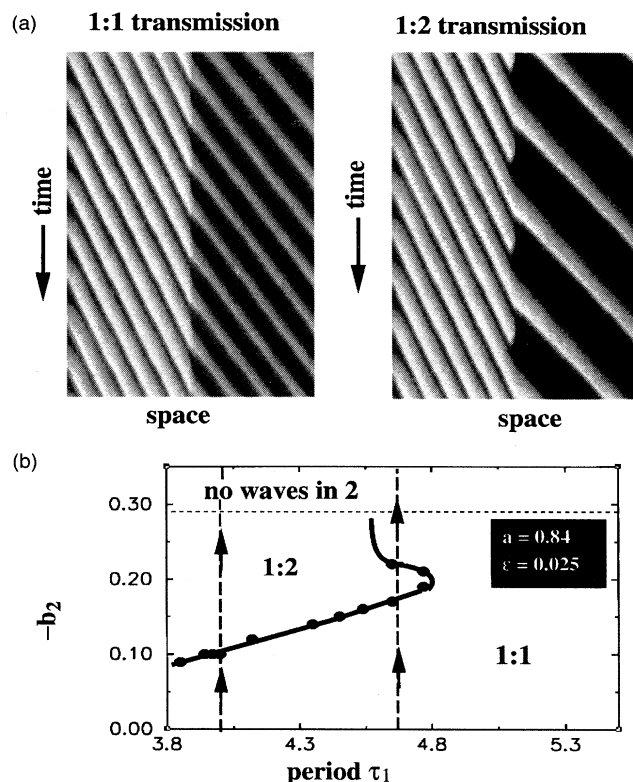


FIG. 1. One-dimensional simulations of a wave train crossing the boundary between media with different kinetic properties. (a) 1:1 transmission at conditions  $a=0.84$ ,  $\epsilon=0.025$ ,  $b_1=0.155$ , and  $b_2=-0.10$ ; 1:2 transmission at  $a=0.84$ ,  $\epsilon=0.025$ ,  $b_1=0.155$ , and  $b_2=-0.12$ . The length of the system is 100 space units, the period of the wave trains in the left half 3.95 time units for both images. All units are dimensionless. (b) Existence region for the two different types of behavior; plotted is  $\tau_1$  against  $b_2$ . Note that a period of 3.8 time units corresponds to  $b_1=0.21$ , whereas a period of 5.4 time units stems from  $b_1=0.00$ . The vertical dashed lines with the arrows show the cuts, which have been investigated in two dimensions.

In 2D, spiral waves naturally provide a source of wave trains without the need for a special boundary condition (different from zero-flux-conditions). To achieve a meaningful comparison with the results in 1D, we produced spiral waves with spontaneous frequency comparable to the 1D-source frequency ( $b_1=0.155$  with  $\tau_1=3.95$ ). We also tried a different example ( $b_1=0.07$  with  $\tau_1=4.68$ ) where the spiral frequency was forced to precisely the 1D-source frequency through the pinning of the spiral to an artificial core [11]. The cuts are visible in Fig. 1(b) as the vertical dashed line with the arrows. In all cases, the 1:1 behavior of the 1D case reappears in 2D leading to patterns like those in Fig. 2(a). The 2D behavior corresponding to the 1:2 wave transmission, however, is far more complex and sensitive: Only when pulses but no spirals are supported by medium 2 individually, do we find the 2D analog of the 1:2 behavior [Fig. 2(b)]. In most cases, two further distinct scenarios emerge involving the “incomplete” blocking of every second wave. The possible final stages of this process include two or more spirals located close to the boundary that suppress the original

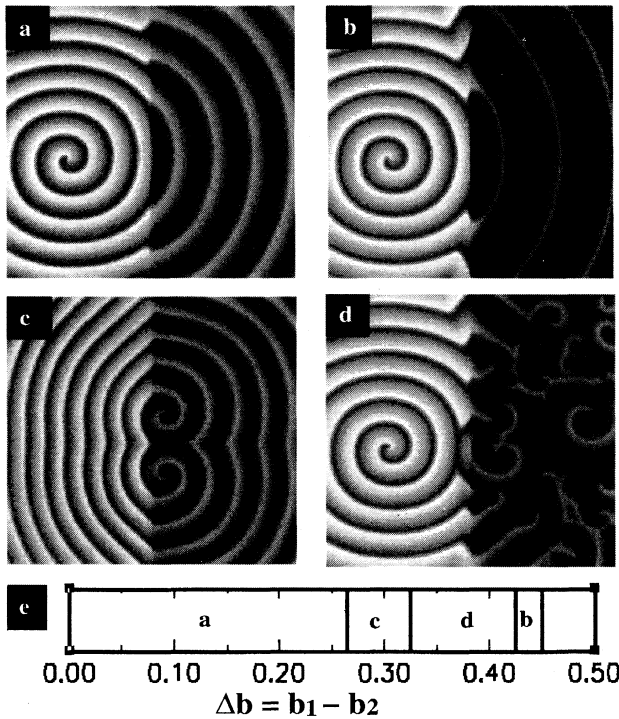


FIG. 2. Examples for possible end state of an initial spiral that sends waves towards a boundary. The parameters  $a=0.89$ ,  $\epsilon=0.025$ , and  $b_1=0.155$  are the same in all cases. (a) 1:1 transmission ( $b_2=-0.10$ ); (b) 1:2 transmission ( $b_2=-0.28$ ); (c) new spirals close to the boundary suppress the original spiral ( $b_2=-0.12$ ); (d) chemical turbulence in medium 2 (right) forced by the spiral to the left in medium 1 ( $b_2=-0.195$ ). The size of all pictures is 100 space units  $\times$  100 space units; (e) regions of behavior in dependence on the magnitude of the step change  $\Delta b=b_1-b_2$ , the letters refer to (a)–(d) as possible end states. For  $\Delta b>0.45$  waves cease to propagate in medium 2.

source in the left half [Fig. 2(c)] and a state of wave disorder in the right half [Fig. 2(d)]. Figure 2(e) summarizes the findings and shows the intervals of different dynamics as a function of the property step change  $\Delta b=b_1-b_2$ . The experimental examples (Figs. 15 and 16 of Ref. [9], respectively) cited above may be representative of two of the scenarios [1:1 transmission in Fig. 2(a) and creation of spiral boundary spirals in Fig. 2(c)] found in the simulations.

Examples of the dynamics leading to creation of new spirals (turbulence) in medium 2 are shown in Figs. 3(a) [3(b)]. In both cases blocking of the wave leads to the formation of open ends that evolve into spiral waves (visible in frame 2 of Fig. 3(a) [in frame 3 of Fig. 3(b)]). If the spontaneous spiral period in medium 2 is smaller than that in medium 1 ( $\tau_{S_2}<\tau_{S_1}$ ), the new spirals generated from the curling of the open ends eventually suppress the original spiral and a pattern governed by two [frame 10 of Fig. 3(a)] or more spirals close to the boundary is observed. Note that the original spiral in Fig. 3(a) moves to the left side and out of bounds as the waves from the higher frequency spirals at the boundary reach its core [frames 8 and 9 in Fig. 3(a)]. This is in accordance with results on competing wave sources in the Belousov-Zhabotinsky reaction [14]. In the second case,

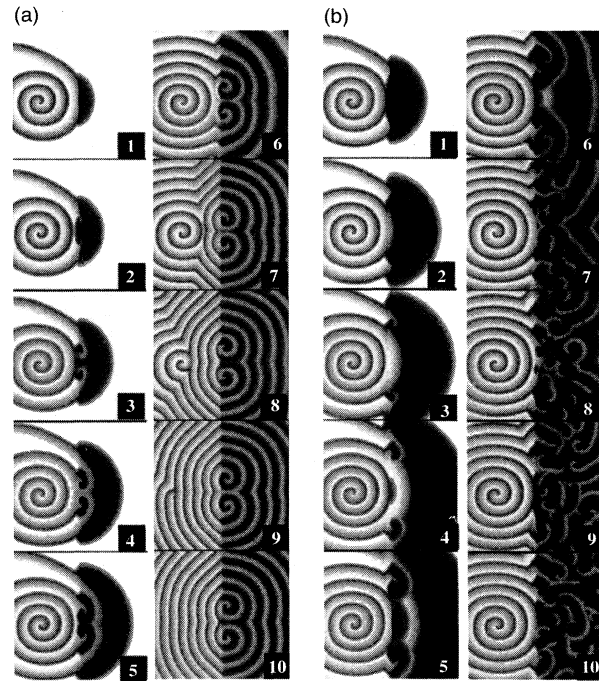


FIG. 3. Temporal evolution of (a) the state in Fig. 2(c) (the time differences between the frames 1 to 5 is 1.34 time units and between frames 5 to 10 it is 80.2 time units) and (b) the state in Fig. 2(d) (the time differences between the frames 1 to 5 is 1.74 time units and between frames 5 to 10 it is 80.2 time units). The spiral period in medium 1,  $\tau_{S_1}$ , is 3.95 time units, in medium 2 its value  $\tau_{S_2}$  amounts to 3.30 time units in (a) and 4.41 time units in (b).

when the spontaneous spiral period in medium 2 is bigger than that in medium 1 ( $\tau_{S_2}>\tau_{S_1}$ ), the new spirals created near the boundary never become stable: they are periodically forced by waves arriving at the boundary from the original spiral source. In addition, there is extensive wave interaction in medium 2 after the breakup at the boundary leading to a complicated “turbulent” pattern. The result in this case is an overall spatiotemporally chaotic state in medium 2 [frame 10 in Fig. 3(b)] that shows typical features of defect mediated turbulence [15], such as the spontaneous creation and mutual annihilation of spiral pairs. This turbulent state is of course different from intrinsic turbulence arising, for example, from spiral breakup in a homogeneous domain, observed in Eqs. (1)–(3) for much bigger values of  $\epsilon$  [16].

Overall, the paradigm of a simple straight boundary between grains reveals a great wealth of interesting dynamic phenomena. The spatial change in medium properties acts as a perturbation on the waves, which must adapt its speed and form to the new medium. The two main findings from this work for a linear “grain boundary” are (a) the possible blocking of plane waves and (b) the creation of spirals close to the boundary, which partially obstructs curved wave propagation through it. Depending on the frequency of these new spirals, they may suppress the original spiral or organize in a turbulent state which is in essence periodically forced by the waves entering the new medium. More results can be expected from composites with more complicated geometries (e.g., periodic media), gradual boundaries, or grains

with strongly varying diffusion coefficients. The study of systems of composite nature should extend the insights in the role of reaction-diffusion waves in biological systems and the understanding of the kinetics of composite catalytic surfaces.

We want to acknowledge financial support by the Deutsche Forschungsgemeinschaft (M.B.) and National Science Foundation (I.G.K.). M.B. and I.G.K. thank the Center of Nonlinear Studies at Los Alamos National Laboratory for its generous hospitality.

- 
- [1] J. D. Murray, *Mathematical Biology* (Springer, Berlin, 1989); H. Meinhardt, *Rep. Prog. Phys.* **55**, 797 (1992); M. C. Cross and P. C. Hohenberg, *Rev. Mod. Phys.* **65**, 851 (1993); A. T. Winfree, *Science* **266**, 1003 (1994).
- [2] J. X. Xin, *J. Stat. Phys.* **73**, 893 (1993); P. Schütz, M. Bode, and H.-G. Purwins, *Physica D* **82**, 382 (1995).
- [3] A. M. Zhabotinsky, M. D. Eager, and I. R. Epstein, *Phys. Rev. Lett.* **71**, 1526 (1993).
- [4] J. Maselko and K. Showalter, *Physica D* **49**, 21 (1991); J. P. Voroney, master's thesis, University of Guelph, 1995 (unpublished); J. P. Voroney, A. Lawniczak, and R. Kapral (unpublished).
- [5] J. J. Tyson and J. P. Keener, *Physica D* **32**, 327 (1988); E. Meron, *Phys. Rep.* **218**, 1 (1992); A. T. Winfree, *Chaos* **1**, 303 (1991).
- [6] A. M. Pertsov, E. A. Ermakova, and E. E. Shnol, *Physica D* **63**, 333 (1990); A. Toth, V. Gaspar, and K. Showalter, *J. Phys. Chem.* **98**, 522 (1994).
- [7] M. Graham, I. G. Kevrekidis, K. Asakura, J. Lauterbach, K. Krischer, H. H. Rotermund, and G. Ertl, *Science* **264**, 80 (1994); K. Agladze, J. P. Keener, S. C. Müller, and A. Panfilov, *ibid.* **264**, 1746 (1994); C. Elphick, A. Hagberg, and E. Meron, *Phys. Rev. E* **51**, 3052 (1995).
- [8] K. Asakura, J. Lauterbach, H. H. Rotermund, and G. Ertl, *Phys. Rev. B* **50**, 8043 (1994).
- [9] K. Asakura, J. Lauterbach, H. H. Rotermund, and G. Ertl, *J. Chem. Phys.* **102**, 8175 (1995).
- [10] W. Engel, M. E. Kordesch, H. H. Rotermund, S. Kubala, and A. von Oertzen, *Ultramicroscopy* **36**, 148 (1991).
- [11] M. Bär, N. Gottschalk, M. Eiswirth, and G. Ertl, *J. Chem. Phys.* **100**, 1202 (1994).
- [12] D. Barkley, *Physica D* **49**, 61 (1991); *Phys. Rev. Lett.* **68**, 2090 (1992).
- [13] D. R. Chialvo and J. Jalife, *Nature* **330**, 749 (1987); C. Elphick, E. Meron, and E. A. Spiegel, *Phys. Rev. Lett.* **61**, 496 (1988).
- [14] V. I. Krinsky and K. I. Agladze, *Physica D* **8**, 50 (1983).
- [15] P. Couillet, L. Gil, and J. Lega, *Phys. Rev. Lett.* **62**, 1619 (1989); M. Hildebrand, M. Bär, and M. Eiswirth, *ibid.* **75**, 1503 (1995).
- [16] M. Bär and M. Eiswirth, *Phys. Rev. E* **48**, R1635 (1993).

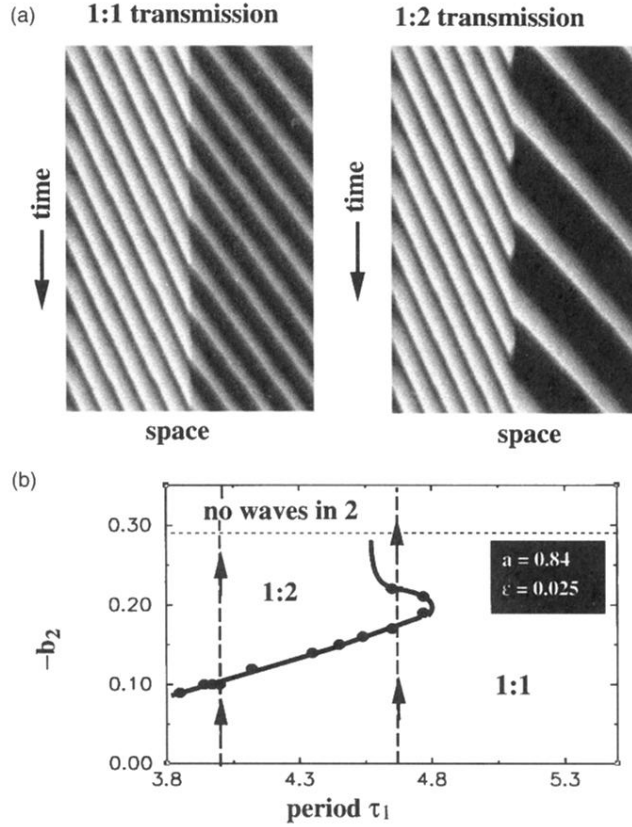


FIG. 1. One-dimensional simulations of a wave train crossing the boundary between media with different kinetic properties. (a) 1:1 transmission at conditions  $a=0.84$ ,  $\epsilon=0.025$ ,  $b_1=0.155$ , and  $b_2=-0.10$ ; 1:2 transmission at  $a=0.84$ ,  $\epsilon=0.025$ ,  $b_1=0.155$ , and  $b_2=-0.12$ . The length of the system is 100 space units, the period of the wave trains in the left half 3.95 time units for both images. All units are dimensionless. (b) Existence region for the two different types of behavior; plotted is  $\tau_1$  against  $b_2$ . Note that a period of 3.8 time units corresponds to  $b_1=0.21$ , whereas a period of 5.4 time units stems from  $b_1=0.00$ . The vertical dashed lines with the arrows show the cuts, which have been investigated in two dimensions.

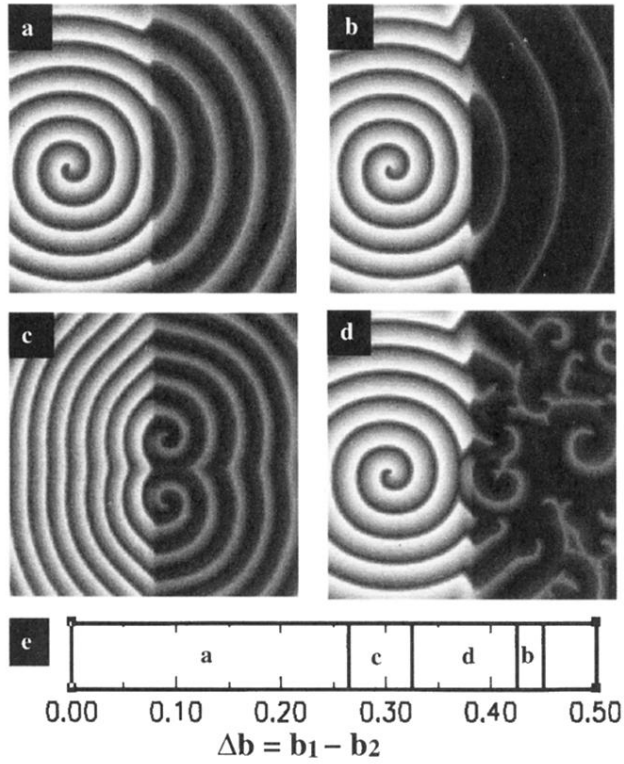


FIG. 2. Examples for possible end state of an initial spiral that sends waves towards a boundary. The parameters  $a=0.89$ ,  $\epsilon=0.025$ , and  $b_1=0.155$  are the same in all cases. (a) 1:1 transmission ( $b_2=-0.10$ ); (b) 1:2 transmission ( $b_2=-0.28$ ); (c) new spirals close to the boundary suppress the original spiral ( $b_2=-0.12$ ); (d) chemical turbulence in medium 2 (right) forced by the spiral to the left in medium 1 ( $b_2=-0.195$ ). The size of all pictures is 100 space units  $\times$  100 space units; (e) regions of behavior in dependence on the magnitude of the step change  $\Delta b=b_1-b_2$ , the letters refer to (a)–(d) as possible end states. For  $\Delta b>0.45$  waves cease to propagate in medium 2.

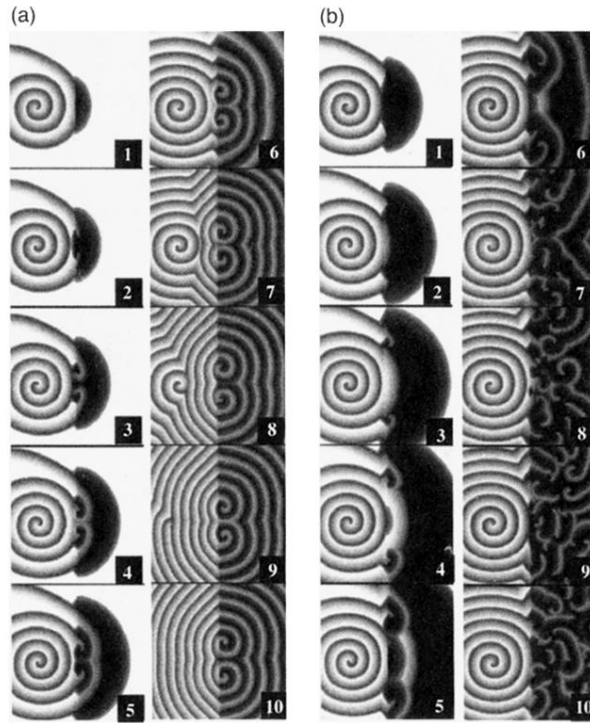


FIG. 3. Temporal evolution of (a) the state in Fig. 2(c) (the time differences between the frames 1 to 5 is 1.34 time units and between frames 5 to 10 it is 80.2 time units) and (b) the state in Fig. 2(d) (the time differences between the frames 1 to 5 is 1.74 time units and between frames 5 to 10 it is 80.2 time units). The spiral period in medium 1,  $\tau_{S_1}$ , is 3.95 time units, in medium 2 its value  $\tau_{S_2}$  amounts to 3.30 time units in (a) and 4.41 time units in (b).